RESEARCH

Observation of Alfvén Waves in an ICME-HSS Interaction Region

Omkar Dhamane[1] · Anil Raghav[1] · Zubair Shaikh[2] · Utsav Panchal[1] · Kalpesh Ghag[1] · Prathmesh Tari[1] · Komal Choraghe[1] · Ankush Bhaskar[3] · Daniele Telloni[4] · Wageesh Mishra[5]

Abstract
The Alfvén wave (AW) is the most common fluctuation present within the solar wind emitted from the Sun. Whether or not AWs can originate after the collision of an Interplanetary Coronal Mass Ejection (ICME) and a High-Speed Stream (HSS) remains an open question. To find an answer to this question, we have investigated an ICME-HSS interaction event observed on 21st October 1999 at 1 AU by the WIND spacecraft. We have used the Walén test to identify AWs and estimated the Elsässer variables to find its characteristics. We explicitly find dominant sunward AWs within the ICME, whereas the trailing HSS has strong anti-sunward AWs. We suggest that the ICME-HSS interaction deforms the Magnetic Cloud (MC) of the ICME, resulting in the generation of AWs inside the MC. Additionally, the existence of reconnection within the ICME's early stage could also contribute to the origin of AWs within it.

Keywords Coronal mass ejection (CME) · High speed stream (HSS) · Alfvén wave

1. Introduction

A coronal mass ejection (CME) is a massive expulsion of a considerable volume of plasma with immense energy flows from the solar corona (Hundhausen, 1999; Webb and Howard, 2012). CMEs, High-speed stream (HSS), and Corotating interaction regions (CIRs) are the primary sources of severe space-weather conditions in the heliosphere and planetary environments (Tsurutani et al., 2006a,b; Schrijver and Siscoe, 2010). A CME's relative excess

✉ A. Raghav
anil.raghav@physics.mu.ac.in

[1] Department of Physics, University of Mumbai, Vidyanagari, Santacruz (E), Mumbai 400098, India

[2] Indian Institute of Geomagnetism (IIG), New Panvel, Navi, Mumbai 410218, India

[3] Vikram Sarabhai Space Centre (VSSC), Indian Space Research Organisation (ISRO), Thiruvananthapuram, Kerala 695022, India

[4] National Institute for Astrophysics, Astrophysical Observatory of Torino, Via Osservatorio 20, I-10025 Pino Torinese, Italy

[5] Indian Institute of Astrophysics, II Block, Koramangala, Bengaluru 560034, India

speed over the ambient solar-wind speed forms the shock front and sheath region (Tsurutani et al., 1988, 2011b; Kilpua, Koskinen, and Pulkkinen, 2017). Fast-forward shocks generate upstream of the CME, i.e., ahead of the solar-origin plasma and field structures (Kennel, Edmiston, and Hada, 1985; Tsurutani et al., 2011b). When a CME moves from the near-Sun region to the interplanetary medium, its kinematic configuration possibly evolves (Vršnak et al., 1993). ICMEs are the Interplanetary counterparts of CMEs observed in the heliosphere using in-situ data. ICMEs cause extreme geomagnetic storms and disruption in the heliosphere and magnetosphere (Tsurutani et al., 1992; Zurbuchen and Richardson, 2006; Echer, Gonzalez, and Tsurutani, 2008; Zhao and Dryer, 2014; Kilpua et al., 2017; Meng, Tsurutani, and Mannucci, 2019). Their hazardous impacts on Earth's space weather are complex for current spacecraft technology to handle (National Research Council, 2008). ICME research has received a lot of interest due to its importance in scientific and technical implications (Schrijver and Siscoe, 2010; Webb and Howard, 2012; Cannon et al., 2013).

The solar wind was first referred to as the phenomenological "solar corpuscular radiation" that causes geomagnetic and auroral activity (Parker, 1965). Generally, it is distinguished into two classes: fast solar wind (speed > 400 km s^{-1}) and slow solar wind (speed < 400 km s^{-1}) (Belcher and Davis Jr, 1971; Dasso et al., 2005; Feldman, Landi, and Schwadron, 2005; Abbo et al., 2016; Tsurutani and Hajra, 2022). The wind's speed is not the only parameter to differentiate between the two, but their relative composition also characterizes the steady bulk plasma properties (Von Steiger et al., 2000). The fast solar wind originates from coronal holes (CHs) in the Sun (Krieger, Timothy, and Roelof, 1973; Gosling and Pizzo, 1999; Vršnak, Temmer, and Veronig, 2007). In addition, data from Ulysses indicates that coronal hole high-speed streams move at a speed of $750 - 800$ km s^{-1} (Balogh et al., 1995; Mann and Kimura, 2000). When an ICME travels in the heliosphere through the solar wind, their interaction, particularly with HSSs, can significantly affect the ICME's properties. This results in the ICME's embedded flux rope to bend, kink, rotate, or become distorted (Riley and Crooker, 2004; Manchester IV et al., 2004; Wang et al., 2006). Sometimes, the flux rope gets eroded due to reconnection in the ICME-HSS interaction (Dasso et al., 2006; Ruffenach et al., 2012; Lavraud et al., 2014; Ruffenach et al., 2015).

The solar wind, particularly the HSS, is characterized by large amplitude Alfvén waves (Belcher and Davis Jr, 1971; Tsurutani et al., 1995a, 1996, 2017, 2018). It is a primary fluctuation in a magnetized plasma, notably incompressible magnetohydrodynamic (MHD) waves (Alfvén, 1942). Due to their distinct properties, Alfvénic oscillations have been regarded as the best MHD mode for energy transport (Alfvén and Lindblad, 1947; Mathioudakis, Jess, and Erdelyi, 2013). The Sun is considered the primary source of AWs (Belcher and Davis Jr, 1971). It is hypothesized that the magnetic reconnection or catastrophe processes that occur during the onset of a CME may result in the generation of low-frequency, anti-sunward AWs and fast- and slow-mode magnetoacoustic waves (Kopp and Pneuman, 1976; Antiochos, DeVore, and Klimchuk, 1999; Chen and Shibata, 2000). However, sunward propagating AWs indicate their generation in interplanetary space. The origin of such AWs is associated with several physical processes, such as: magnetic reconnection exhausts (Belcher and Davis Jr, 1971; Gosling et al., 2009), backstreaming ions from reverse shocks (Gosling, Tian, and Phan, 2011), steepening of a magnetosonic wave (Tsurutani et al., 2011b, 1988), interaction of multiple CMEs (Raghav and Kule, 2018), etc. It has been proposed that AWs are produced locally by velocity shear instabilities caused by their interaction with high-velocity streams (Coleman Jr, 1968; Bavassano, Dobrowolny, and Moreno, 1978; Roberts et al., 1987, 1992). Besides, AWs are locally generated due to kinetic instabilities linked to the solar-wind proton heat flux (Neugebauer, 1981). According to models of the expanding solar wind by Matteini et al. (2006), and Hellinger and Trávníček (2008), the plasma is unstable to the firehose

and oblique firehose instabilities at a distance of about 1 AU. Intriguingly, oblique AWs are produced by the firehose instability. Additionally, the solar wind expansion increases the ratio of differential particle velocity to local Alfvén speed, which leads to the oblique AWs instability (Hellinger and Trávníček, 2011, 2013).

AWs play a crucial role in both the dynamics of the Earth's magnetosphere and the study of space plasmas in astrophysics (e.g., Cummings, O'sullivan, and Coleman Jr, 1969; Singer et al., 1981; Tsurutani and Gonzalez, 1987; Hui and Seyler, 1992; Johnson and Cheng, 1997; Lysak, 2004, and references therein). Tsurutani and Gonzalez (1987) claimed that high-intensity long-duration continuous auroral activity (HILDCAA) events are caused by outward (from the Sun) propagating interplanetary AW trains. The HSSs contain AWs linked to HILDCAA events (Tsurutani et al., 2011a). Moreover, Chaston et al. (2007) hypothesized that auroral particles can be accelerated by AWs. The Alfvénic fluctuations or AWs can affect the ionosphere, resulting in various phenomena (Verkhoglyadova et al., 2013). The ponderomotive force generated by an AW can create a cavity into the ionospheric plasma (Bellan and Stasiewicz, 1998). Chaston et al. (2006) hypothesized that AWs cause ionosphere erosion. Hull et al. (2019) suggested that the dispersive AWs become quite essential in energising O^+ ions in the inner magnetosphere. Moreover, during geomagnetic storms, the Alfvénic fluctuations inside the ICME substructures can cause the extended recovery of the geomagnetic field (Raghav et al., 2018; Raghav, Choraghe, and Shaikh, 2019; Shaikh et al., 2019; Telloni et al., 2021). Besides, it was also shown that during the storm's main phase, the hemisphere's Alfvénic power surged four times when compared to non-storm periods (Keiling et al., 2019). In addition, AWs play a significant role in plasma heating (Hasegawa and Chen, 1974), transportation (e.g., Hasegawa and Chen, 1975; Chen and Zonca, 2016, and references therein), magnetotail dynamics (Keiling, 2009), auroral dynamics (Stasiewicz et al., 2000), etc. Therefore, it is important to investigate the origin and propagation of the AW and its related processes.

The structural configuration of large-scale magnetic structures is altered by interactions, such as CME-CME, CME-HSS, CME-CIR, etc. Heinemann et al. (2019) showed the signature of a Stream interface (SI) as the HSS passes the slow solar wind, resulting in a drop in proton density and a sharp increase in temperature. They further pointed out that the HSS follows the CME, and their interaction gives a sharp rise in the magnetic field, proton density, velocity, and temperature corresponding to the shock sheath region. Theoretical studies also suggest that when large-scale magnetic structures interact, momentum and energy are transferred in the form of an MHD wave (Jacques, 1977). Raghav et al. (2018) investigated a CME-CME interaction event and discovered torsional AWs in the magnetic cloud (MC) region. Moreover, Alfvénic fluctuations were found in the ICME sheath (Raghav et al., 2022b) and the stream interface of fast and slow solar-wind interaction (Lepping et al., 1997; Tsurutani et al., 1995b). Here, we present the first observation of AWs generation caused by the interaction between the ICME and following HSS.

2. Data, Methods, and Observations

We examined the ICME-HSS interaction event observed by the WIND spacecraft on 21st October 1999. We used 92 sec temporal resolution data of the plasma and magnetic field in GSE coordinates to examine the interplanetary conditions during the passage of the interaction region. Moreover, to determine the presence of AWs, we analysed high-resolution data from WIND's satellite sensors (such as WIND MFI, and 3DP) with a 3 sec resolution. The data is available at wind.nasa.gov/data.php.

2.1. Interplanetary Conditions

The interplanetary conditions during the passage of the ICME-HSS interaction region are demonstrated in Figure 1. A sudden sharp enhancement is observed in the total interplanetary magnetic field (IMF), plasma density, and solar-wind speed, suggesting the onset of the ICME at 02:19 UT on 21 October 1999. The low plasma beta (β) and low fluctuations in the IMF indicate the magnetic cloud (MC) crossover. The electron pitch-angle shows a nearly bidirectional flow that confirms a possible closed magnetic structure. The rear-end is observed at 06:29 UT, on 22 October 1999. There are also signatures of reverse shock on the 24 October 1999 at 03:04 UT, i.e., decrease in magnetic intensity, temperature, and number density (indicated by a dotted magenta line in Figure 1). The ICME boundaries are also confirmed by the ICME catalogue, available at wind.nasa.gov/ICME_catalog/ICME_ catalog_viewer.php

In general, MCs of ICMEs depict a gradual decrease in total IMF and solar-wind speed, which implies the expansion of the MC in the solar wind. However, in the studied event, the trailing edge of the MC demonstrates an anomalous behaviour, such as a rise in the total IMF and solar-wind speed. Thus, it is clearly visible that the observed ICME's MC completely contradicts the conventional definition of a MC. The anomalous behaviour at the trailing edge of the ICME's MC could be due to the existence of a HSS flow from behind. The compression of the ICME's MC by the HSS causes the plasma particles to pile up at the trailing end, along with the high IMF fluctuations (Rodriguez et al., 2016). The temperature and density rise at the interface between an ICME and HSS causes thermal pressure to rise as well. As a result, the force balance conditions of the ICME flux rope may be altered. Hence, we believe that the MC is distorted due to the ICME-HSS interaction and the corresponding HSS may cause turbulence at the rear end of the MC. Additionally, at the leading part of the ICME, we observe two sharp dips in the total magnetic field, which coincide with a rise in proton density, alpha density and plasma temperature. This can be interpreted as magnetic reconnection exhaust, based on reported literature (Gosling et al., 2005).

2.2. Alfvén Wave Identification

AWs are the most basic form of fluctuation in a magnetic plasma, commonly identified in the solar wind across the heliosphere (Alfvén, 1942; Belcher and Davis Jr, 1971). The Alfvén velocity fluctuations ΔV_A are defined as,

$$\Delta V_A = \frac{\Delta B}{\sqrt{\mu_0 \rho}}, \tag{1}$$

where, $\Delta B = B - B_{avg}$ are the fluctuations in the respective components of the IMF. A correct assessments of the fluctuations magnitude requires the accurate estimate of background values. In the literature, a precise de Hoffmann-Teller frame or mean values are utilized as a background value to diagnose the existence of interplanetary AWs (Gosling et al., 2009; Yang and Chao, 2013; Raghav and Kule, 2018; Raghav et al., 2018). However, in an HSS, the HT frame might vary rapidly (Gosling et al., 2009; Li et al., 2016), and the use of an average value as the background state is not always appropriate. As a result, during the examined ICME-HSS interaction, we employed other techniques to identify large-amplitude AWs. The entire data set being analyzed is divided into ten-minute time intervals. Each time window's data is passed through the 4th order Butterworth filter (using MATLAB software). We choose 10 periodic bands for bandpass filter: $10 - 15$ sec, $15 - 25$ sec, $25 - 40$ sec,
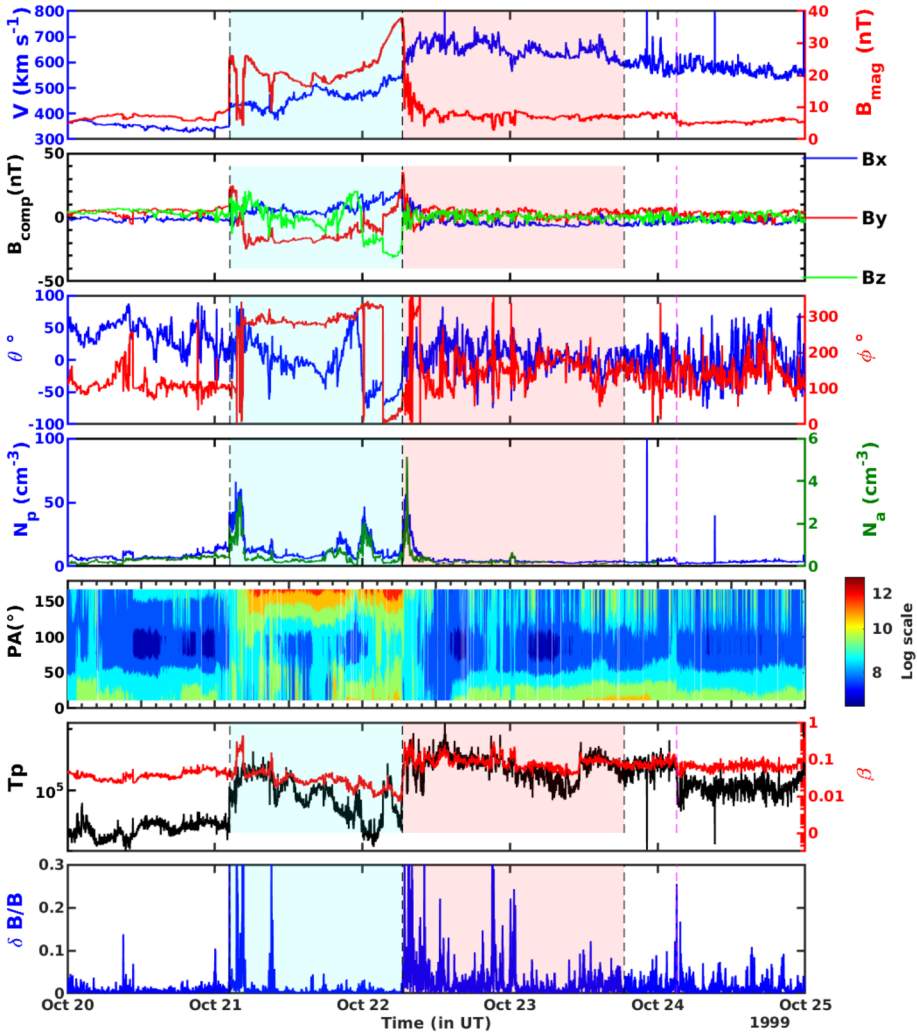
Figure 1 WIND observation of complex ICME–HSS interaction event on 1999 October 20–24 (time cadence of 92 sec) Total interplanetary field strength IMF B_{mag} in nT and total solar wind V (km s^{-1}) are shown in the top panel. The components of the magnetic field are shown in the second panel. The third panel displays the IMF orientation (θ, ϕ). In the fourth panel, the proton number density (N_p) is represented on the left, while alpha density N_a is shown on the right. The pitch angle (PA) of superthermal electron strahls is depicted in the fifth panel. The proton temperature (T_P) and the β value were plotted in the sixth panel on the left- and right- sides, respectively. The plot of $\delta B/$B is demonstrated in last panel.

40 – 60 sec, 60 – 100 sec, 100 – 160 sec, 160 – 250 sec, 250 – 400 sec, 400 s – 630 sec, and 630 – 1000 sec in an evenly distributed manner. In our study, the AWs are observed in frequency bands between 10^{-3} to 10^{-1} Hz. The Walén relation is used to determine the relationship between the Alfvén and the solar-wind velocity components as,
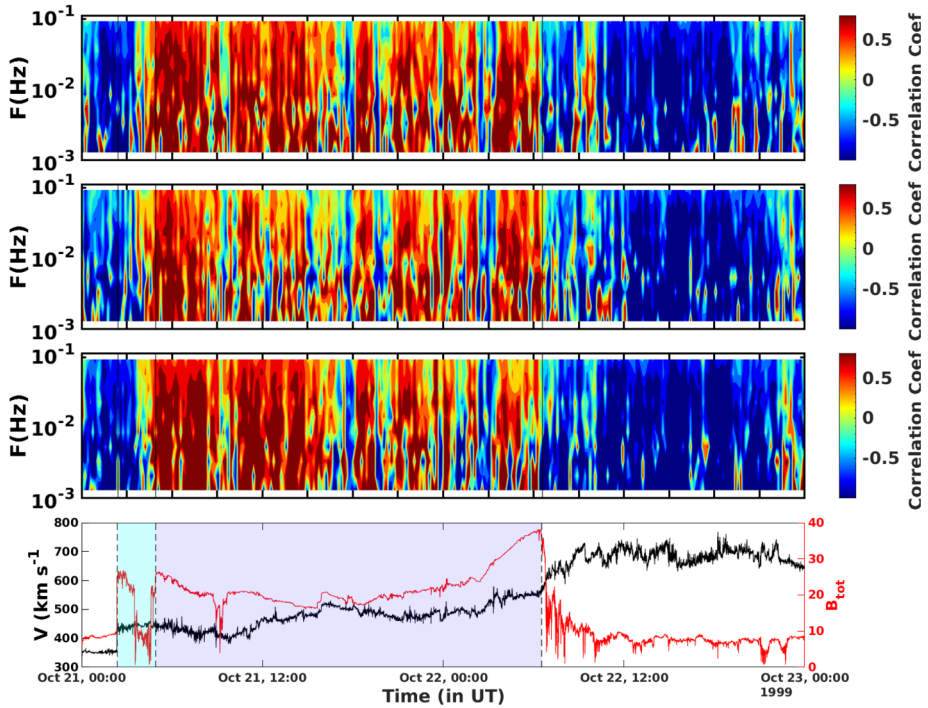
$$\Delta V_i = |R_{wi}| \, \Delta V_{Ai}, \qquad (2)$$

Figure 2 In the time-frequency domain, the correlation coefficients between V_{Ai} and V_i for the ICME-HSS event are presented. The top three panels show the correlation coefficient for x, y, and z components, respectively. The bottom panel shows the total magnetic field (B_{mag}), and solar-wind velocity (V) is plotted for reference. The shaded region in the bottom panel depicts ICME region.

where R_{wi} is known as the Walén slope which represent the linear relationship between ΔV_{Ai} and ΔV_i. Furthermore, the presence of AWs or Alfvénic fluctuations in the examined region was demonstrated by the Pearson correlation coefficient between the respective components of ΔV_i and ΔV_{Ai}. Figure 2 demonstrates the existence of AWs during the ICME-HSS interaction. The colour bar shows the correlation coefficient between the components of ΔV_A and ΔV. Here, correlation coefficient $= -1$ (dark-blue shade) implies the existence of anti-sunward AWs, whereas correlation coefficient $= 1$ (dark-red shade) means sunward AWs. The top three panels show the frequency-dependent distribution of correlation coefficient between the respective components (x, y, and z) of ΔV_A and ΔV. A negative correlation coefficient was observed at the ICME upstream solar wind and trailing HSS region. In contrast, during the ICME transit, we mainly observed a positive correlation coefficient. This implies the ICME is superimposed with the dominant sunward AWs, whereas the trailing HSS shows anti-sunward flow.

Figure 3 depicts the correlation analysis between the respective components of ΔV and ΔV_A for ICME's MC. We used the 4th order butter-worth MATLAB filter algorithm with a single broadband frequency boundary of 10^{-3} to 10^{-1} Hz to filter the ΔV data and ΔV_A components. We found the Pearson correlation coefficients for each x, y, and z component were 0.44, 0.98, and 0.86, respectively. The strong positive correlation confirmed the sunward nature of the AWs in the studied ICME's MC region.
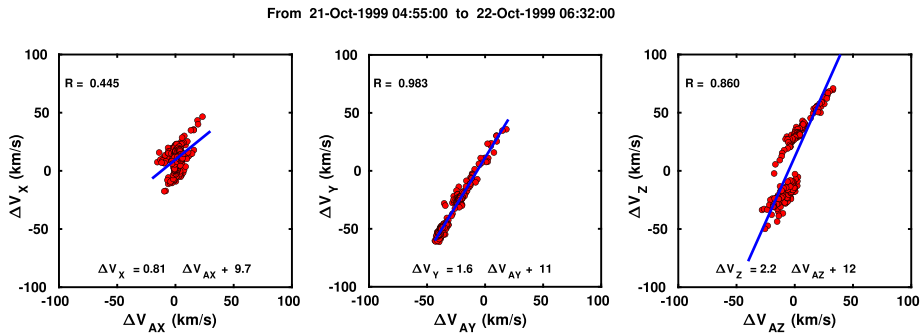
From 21-Oct-1999 04:55:00 to 22-Oct-1999 06:32:00

Figure 3 Analysis of the correlation between the corresponding ΔV and ΔV_A components. The scattered black circle with filled red colour represents the WIND spacecraft observations with a time cadence of 3 sec. The coefficient of correlation is denoted by R. Each panel shows the linear fit relationship between the corresponding components of ΔV and ΔV_A.

2.3. Characteristics of the Alfvén Waves

Generally, Elsässer variables are used to characterize the solar-wind turbulence and AW properties (Elsasser, 1950; Marsch and Mangeney, 1987; Bruno and Carbone, 2013a). Here, we employed them to distinguish the dominant flow of outward and inward Alfvénic fluctuations (Elsasser, 1950; Marsch and Mangeney, 1987; Bruno and Carbone, 2013a). The Elsässer variables are defined as

$$Z^{\pm} = V \pm \frac{B}{\sqrt{4\pi\rho}}. \tag{3}$$

Here, V and B are fluctuations in the proton velocity and magnetic field, respectively. The $\pm$ sign in front of B depends on the sign of $[-k \cdot B_0]$, where k is a wave vector. If both the velocity and magnetic field are directed outward, Equation 3 manifests as $Z^+ = V - V_A$ and $Z^- = V + V_A$. On the other hand, if the magnetic field points in the direction towards the Sun, the correlation sign is reversed (V points always outwards), and $Z^+ = V + V_A$ and $Z^- = V - V_A$ are the results. In this sense, Z^+ and Z^- represent outward and inward Alfvénic modes, respectively, at all times. (Roberts et al., 1987; Bruno and Bavassano, 1991; D'Amicis and Bruno, 2015)

Figure 4 represents the characteristics of the AWs in question. The top three panels clearly show that components of ΔV and ΔV_A are either correlated or anti-correlated. This implies that the existence of AWs in the studied region exhibits both outward and inward propagation nature. In order to gain a better clarity on the time evolution of outward and inward propagation of the waves, we have demonstrated the ratio Z^-/Z^+, normalized cross helicity (σ_c), the angle between ΔV and ΔB (θ_{VB}), and the normalized residual energy (σ_R) in Figure 4.

We find a mean value of the ratio of Elsässer variables of ~ 0.54 in the HSS region, whereas it is ~ 2.13 inside the ICME's MC. In fact, the temporal fluctuation in the ratio reached ~ 10 in the anterior part of the MC and highly varies in the trailing part of the MC.

The normalized cross helicity (σ_c) is defined as,

$$\sigma_c = \left(\frac{e^+ - e^-}{e^+ + e^-}\right), \tag{4}$$

where $e^{\pm} = \frac{1}{2}(z^{\pm})^2$, e^- and e^+ are the energies related to z^- and z^+. The normalized cross helicity shows the degree of Alfvénicity (Tu, Marsch, and Thieme, 1989). Moreover, $\sigma_c \sim 1$ denotes a prominent outward propagating flow whereas $\sigma_c \sim -1$ depicts a dominating inward propagating flow (Matthaeus and Goldstein, 1982; Tu, Marsch, and Thieme, 1989). The analysis yielded a positive average value for the HSS region, i.e., $\sigma_c = 0.57$, indicating predominately outward flow. Furthermore, we observed $\sigma_c = -1$ with high fluctuations in the front part of the MC. Moreover, the mean value for the ICME's MC was found to be $\sigma_c = -0.22$, implying inward flow in the MC region.

To quantify the wave propagation direction, we have estimated the angle (θ_{VB}) between V and B_{mag} as follows:

$$\theta_{VB} = \cos^{-1}(\frac{-B_x}{B_{\mathrm{mag}}}). \tag{5}$$

We frequently observed values of θ below 30°, and the mean value around 40.21° in the HSS region. This implies the two vectors are nearly parallel in the HSS region, supporting the observed strong outward Alfvénic flow. However, in the MC region, we observed highly fluctuating angles, which sometimes reached a value of 150°. The mean value of the angle is observed at 109.67°.

The normalized residual energy is defined as

$$\sigma_R = (\frac{e^v - e^b}{e^v + e^b}), \tag{6}$$

where e^v and e^b are the kinetic and magnetic energies, respectively. σ_R is a measure of the excess magnetic field energy with respect to the kinetic energy or vice versa (Bruno and Carbone, 2013a). Our analysis revealed that the value of σ_R is routinely below 1 in the HSS region, whereas it is highly fluctuating in the MC region, possibly due to the mixing of inward and outward waves.

3. Discussion and Conclusions

Alfvénic fluctuations are transverse magnetohydrodynamic (MHD) fluctuations in which ions and magnetic fields oscillate at low frequencies (Cross, 1988; Cramer, 2001). They propagate in the direction of the magnetic field, with the ion mass density providing inertia and the magnetic field lines providing a restoring tension force. Alfvénic fluctuations are ubiquitous in space plasmas, such as: the ionosphere, the magnetotail (Keiling, 2009), the magnetosheath, the interplanetary space (Wang et al., 2012), the slow solar wind (D'amicis, Matteini, and Bruno, 2019), and fast solar wind (Hollweg, 1975; Tsurutani et al., 2018), co-rotating interaction region (CIR) (Tsubouchi, 2009; Shi et al., 2020), the ICME's sheath (Shaikh, Raghav, and Vichare, 2019) and MC (Raghav et al., 2018), the planetary region (Hinton, Bagenal, and Bonfond, 2019), the inner-heliosphere (Bavassano and Bruno, 1989b; Perrone et al., 2020), the outer-heliosphere, the astrophysical plasma, the solar corona (Tomczyk et al., 2007; Cally, 2017), the solar surface or atmosphere (Jess et al., 2009; Mathioudakis, Jess, and Erdelyi, 2013), the lab-plasma (Gekelman, 1999, 2003). Raghav et al. (2022a) found the existence of surface AWs in the ICME flux rope. The AW shows some peculiar characteristics such as period doubling phenomena, arc polarization and phase steepening (Riley et al., 1996a; Tsurutani et al., 2018; Shaikh, Raghav, and Vichare, 2019).
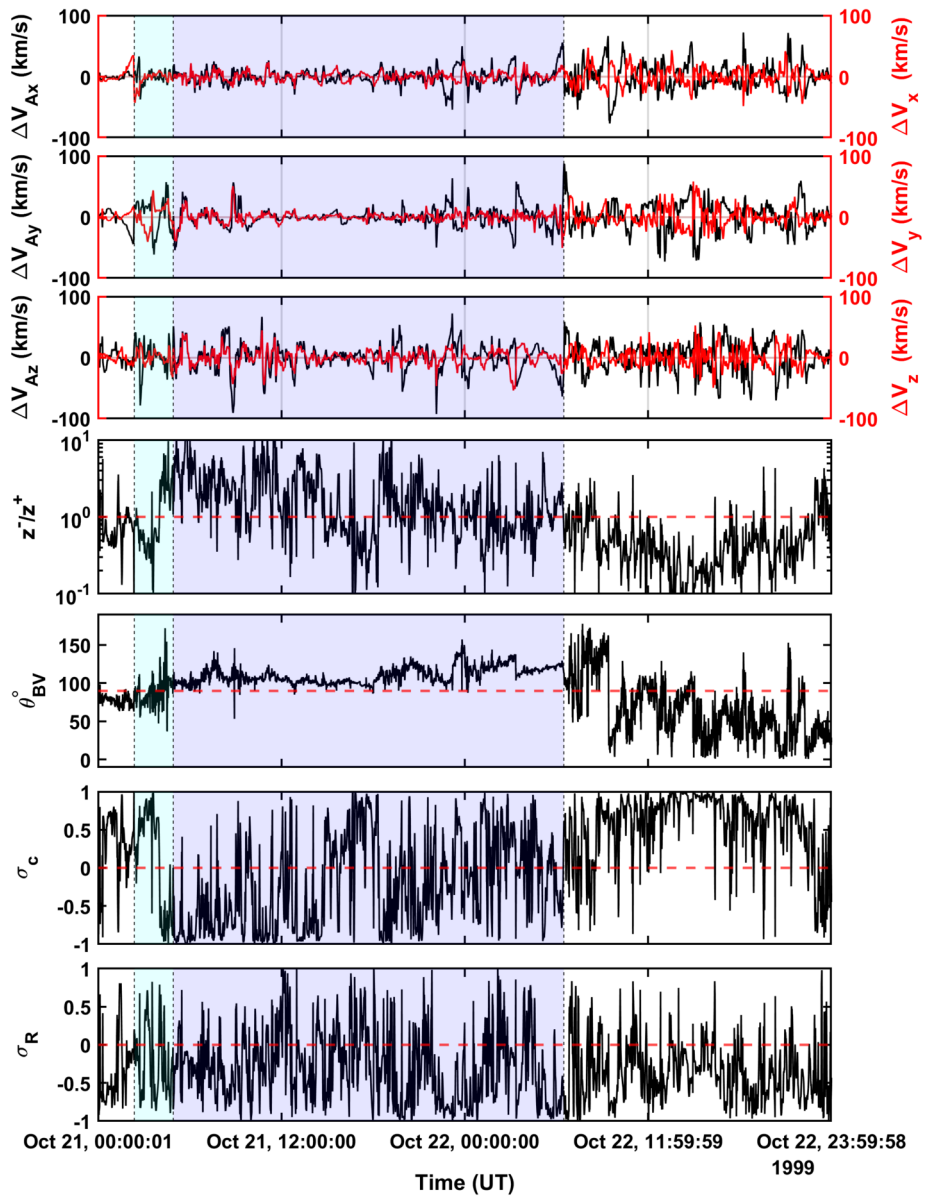
Figure 4 The top three panels compare Alfvén velocity fluctuations ΔV_{Ai} (red) to proton flow velocity fluctuations ΔV_p over time (blue). They demonstrate the Alfvénic features in MC and HSS regions. The ratio of Elsässer variables z^-/z^+ is shown in the fourth panel. The fifth panel depicts the angle between the Alfvén velocity and the solar-wind speed. The bottom two panels show the temporal variation of the normalized cross-helicity (σ_c) and normalized residual energy (σ_R). WIND (MFI and 3DP) spacecraft data are used for the above analysis with a time cadence of 3 sec.

It is worth noting that the outward AWs are widespread in the solar wind, whereas inward AWs are uncommon (Belcher, Davis Jr, and Smith, 1969; Daily, 1973; Burlaga and

Turner, 1976; Riley et al., 1996b; Yang et al., 2016). With growing heliocentric distance, inward AWs are expected. They're also associated with unusual occurrences like magnetic reconnection exhausts and/or back-streaming ions from reverse shocks (Belcher and Davis Jr, 1971; Roberts et al., 1987; Bavassano and Bruno, 1989b; Gosling et al., 2009; Gosling, Tian, and Phan, 2011). Localized superposition of inward and outward AWs may be caused by the solar-wind velocity shear effect, triggered by plasma instabilities (Bavassano and Bruno, 1989a). When both AWs are present simultaneously, non-linear interactions occur (Dobrowolny, Mangeney, and Veltri, 1980), which are essential for the dynamical evolution of a Kolmogorov-like MHD spectrum (Bruno and Carbone, 2013a). In general, the solar wind is uniform and persistent in high latitudes; therefore, a decrease in the cross-helicity could be induced by parametric instability (Malara, Primavera, and Veltri, 2001). The helicity decreases as the heliocentric distance increases (Bavassano, Pietropaolo, and Bruno, 2000; Matthaeus et al., 2004).

Here, we demonstrated the existence of an AW during the ICME-HSS interaction at 1 AU. The observations in Figure 1 indicate that the HSS interacts with the ICME from the trailing edge. In the studied ICME event, we observed the upstream shock with small magnetic field amplitude and very weak sheath region formation. The proton speed of this ICME has diminished in the leading part of the MC region. As a result, the ICME MC has similar characteristics to a slow MC. In the typical case, as referred to above, there would be no forward shock and sheath (Tsurutani et al., 2004). In our case, there is a forward shock and weak/no sheath. But, we observed a reverse shock at the end of the ICME interval (Tsurutani et al., 2011b). The ICME's velocity increased from ~ 460 km s^{-1} to ~ 700 km s^{-1}, indicating that the HSS is dynamically compressing the ICME. The compression intensifies the magnetic field to almost double in magnitude in its rear part, resulting in a strong geomagnetic perturbation (Dal Lago et al., 2006; Singh et al., 2009; Kilpua et al., 2012). As a result, the ICME's MC does not appear to be expanding as expected; rather, the rise in the total IMF near the rear end implies the compression of the MC. In the B_y, B_z, and θ variations, the distortion is clearly visible (Kilpua et al., 2012). Based on the observations and estimations shown in Figure 2 and 4, we explicitly observed the AW during this interaction. From the correlation values and temporal fluctuations in various estimated quantities using Elsässer variables, we infer that the initial part of the ICME's MC superposed with a strong inward AW flow, whereas the HSS region displayed a strong outward flow.

Alfvénic fluctuations in the solar wind are usually a mix of two populations: outward-propagating and inward-propagating (D'Amicis and Bruno, 2015). The Walén slope (or the correlation between the magnetic field and plasma velocity) of AWs observed in the solar wind can be significantly reduced by a mix of inward and outward AWs (Belcher and Davis Jr, 1971; Marsch and Tu, 1993; Bruno and Carbone, 2013b; Yang et al., 2016). The observed AWs lie in the frequency range 10^{-3} to 10^{-1} Hz. Therefore, to verify the temporal variation of correlation coefficient and regression coefficient, we passed the data of V and V_A components through the 4th order Butter-worth MATLAB filter algorithm with a single broadband frequency boundaries of 10^{-3} to 10^{-1} Hz. We divided the data set to be analyzed into ten-minute intervals (200 data points in each interval). Furthermore, we estimated the correlation coefficient and regression coefficient between the respective components of V and V_A for each time window. Figure 5 shows the temporal variation of the correlation coefficient (top panel) and regression coefficient (middle panel) for the observed Alfvénic region. The correlation coefficient and regression coefficient fluctuate to ~ -1 in the HSS region, corroborating strong outward flow. In contrast, both quantities fluctuate to ~ 1 in the front part of the MC, suggesting the inward flow of Alfvénic fluctuations. However, we found highly fluctuating values for both coefficients and Elsässer variables (see Figure 4)
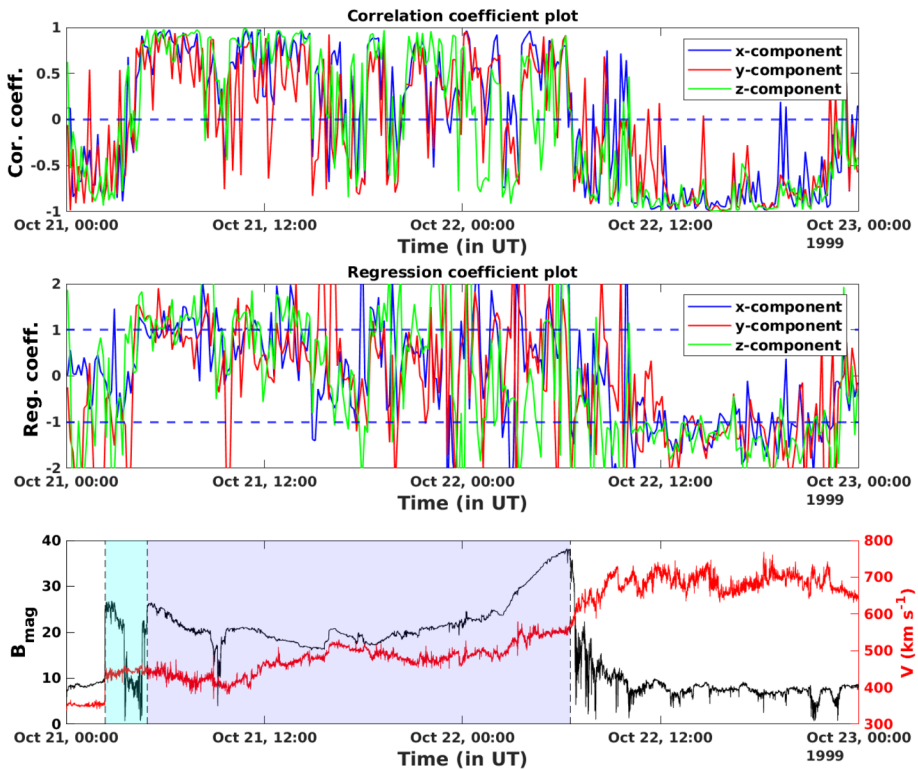
Figure 5 The top and middle panels show the fluctuations in correlation coefficient and the regression coefficient of each component of velocity and magnetic field. The bottom panel references the evolution of the ICME and HSS using B_{mag} and solar-wind speed.

at the trailing part of the MC. In the studied interaction case, the MC's internal (magnetic) pressure increases due to the compression exerted by the HSS. The resulting force sweeps the plasma backward, i.e., the reflection of ions from the rear boundary. Note that the AW's amplitude is lower in the MC's trailing part than in the HSS and front part. Therefore, we believe that the outward and inward AWs are generated or reflected at the rear boundary of the MC. Moreover, the mixing of inward and outward AWs within the trailing part of the MC region is possible, as suggested in the reported studies (D'Amicis and Bruno, 2015). It is exciting to examine the inward-outward interaction region to understand parametric instabilities, which will be studied in the near future.

The generation of the AWs in our study could be attributed to the following reasons: (1) steepening of a magnetosonic wave that generates the shock at the leading edge of the MC (Tsurutani et al., 1988, 2011b). (2) The velocity shear due to the interaction between the ICME and HSS (Bavassano, Dobrowolny, and Moreno, 1978; Roberts et al., 1992; Hollweg and Kaghashvili, 2011). (3) Tsurutani et al. (1988) distinguished the driver gas/MC as regions without AWs or discontinuities. However, AWs are detected, implying that they may be a leak in the MC from the HSS or generated locally. (4) Besides, there was a reverse shock observed on 24th October 1999, which may have some role in the AWs being generated through the backstreaming of ions (Gosling, Tian, and Phan, 2011). (5) Furthermore, the reconnection region observed at the leading edge of the MC (Petschek, 1964; Levy,

Petschek, and Siscoe, 1964; Gosling et al., 2005), and Gosling et al. (2005) suggest that the reconnection exhaust at the heliospheric current sheet (HCS) can generate AWs. (6) Apart from this, a simulation study by Tsubouchi (2009) claimed that the Alfvénic fluctuations in a HSS interact with a velocity gradient structure. The initial AWs break into two Alfvén modes that travel in opposite directions. Here, powerful parallel and antiparallel flows produce the field gradient at the edges, acting as a mirror force to modify the magnetic intensity. Moreover, Wang, Feng, and Zheng (2019) perform multi-spacecraft observations of the MC and suggest that AWs can have unidirectional as well as bidirectional AWs. They also speculated that unidirectional AWs are formed within an MC by distortions in a pre-existing flux rope, while bidirectional AWs are emitted from the centre of reconnection and subsequently move outward along two-foot legs of an ICME flux rope. In our study, it appears that the AWs (inward waves) within the MC could be due to distortions of the MC. This distortion is caused by the HSS. Furthermore, this AW embedded MC travels in the sea of the HSS, which has an outward AW. Thus, our study will be significant in understanding the ICME-solar wind interaction and underlying physical mechanism of these waves.

Declarations

Competing interests The authors declare no competing interests.

References

Abbo, L., Ofman, L., Antiochos, S., Hansteen, V., Harra, L., Ko, Y.-K., Lapenta, G., Li, B., Riley, P., Strachan, L., et al.: 2016, Slow solar wind: observations and modeling. *Space Sci. Rev.* **201**, 55.

Alfvén, H.: 1942, Existence of electromagnetic-hydrodynamic waves. *Nature* **150**, 405.

Alfvén, H., Lindblad, B.: 1947, Granulation, magneto-hydrodynamic waves, and the heating of the solar corona. *Mon. Not. Roy. Astron. Soc.* **107**, 211.

Antiochos, S., DeVore, C., Klimchuk, J.: 1999, A model for solar coronal mass ejections. *Astrophys. J.* **510**, 485.

Balogh, A., Southwood, D., Forsyth, R., Horbury, T., Smith, E., Tsurutani, B.: 1995, The heliospheric magnetic field over the south polar region of the Sun. *Science* **268**, 1007.

Bavassano, B., Bruno, R.: 1989a, Evidence of local generation of Alfvénic turbulence in the solar wind. *J. Geophys. Res., Space Phys.* **94**, 11977.

Bavassano, B., Bruno, R.: 1989b, Large-scale solar wind fluctuations in the inner heliosphere at low solar activity. *J. Geophys. Res., Space Phys.* **94**, 168.

Bavassano, B., Dobrowolny, M., Moreno, G.: 1978, Local instabilities of Alfven waves in high speed streams. *Solar Phys.* **57**, 445.

Bavassano, B., Pietropaolo, E., Bruno, R.: 2000, Alfvénic turbulence in the polar wind: a statistical study on cross helicity and residual energy variations. *J. Geophys. Res., Space Phys.* **105**, 12697.

Belcher, J., Davis, L. Jr: 1971, Large-amplitude Alfvén waves in the interplanetary medium, 2. *J. Geophys. Res.* **76**, 3534.

Belcher, J., Davis, L. Jr, Smith, E.: 1969, Large-amplitude Alfvén waves in the interplanetary medium: Mariner 5. *J. Geophys. Res.* **74**, 2302.

Bellan, P., Stasiewicz, K.: 1998, Fine-scale cavitation of ionospheric plasma caused by inertial Alfvén wave ponderomotive force. *Phys. Rev. Lett.* **80**, 3523.

Bruno, R., Bavassano, B.: 1991, Origin of low cross-helicity regions in the inner solar wind. *J. Geophys. Res., Space Phys.* **96**, 7841.

Bruno, R., Carbone, V.: 2013a, The solar wind as a turbulence laboratory. *Living Rev. Solar Phys.* **10**, 1.

Bruno, R., Carbone, V.: 2013b, Living Rev. *Solar Phys* **10**.

Burlaga, L., Turner, J.: 1976, Microscale 'Alfvén waves' in the solar wind at 1 AU. *J. Geophys. Res.* **81**, 73.

Cally, P.S.: 2017, Alfvén waves in the structured solar corona. *Mon. Not. Roy. Astron. Soc.* **466**, 413.

Cannon, P., Angling, M., Barclay, L., Curry, C., Dyer, C., Edwards, R., Greene, G., Hapgood, M., Horne, R.B., Jackson, D., et al.: 2013, *Extreme Space Weather: Impacts on Engineered Systems and Infrastructure*, Royal Academy of Engineering, London. ISBN 1-903496-95-0.

Chaston, C., Génot, V., Bonnell, J., Carlson, C., McFadden, J., Ergun, R., Strangeway, R., Lund, E., Hwang, K.: 2006, Ionospheric erosion by Alfvén waves. *J. Geophys. Res.: Space Physics* **111**.

Chaston, C., Carlson, C., McFadden, J., Ergun, R., Strangeway, R.: 2007, How important are dispersive Alfvén waves for auroral particle acceleration? *Geophys. Res. Lett.* **34**.

Chen, L., Zonca, F.: 2016, Physics of Alfvén waves and energetic particles in burning plasmas. *Rev. Mod. Phys.* **88**, 015008.

Chen, P., Shibata, K.: 2000, An emerging flux trigger mechanism for coronal mass ejections. *Astrophys. J.* **545**, 524.

Coleman, P.J. Jr: 1968, Turbulence, viscosity, and dissipation in the solar-wind plasma. *Astrophys. J.* **153**, 371.

Cramer, N.F.: 2001, *The Physics of Alfvén Waves*, Wiley, New York. DOI.

Cross, R.: 1988, *An Introduction to Alfven Waves*, A. Hilger, Bristol, England Philadelphia ISBN 9780852742457.

Cummings, W., O'sullivan, R., Coleman, P. Jr: 1969, Standing Alfvén waves in the magnetosphere. *J. Geophys. Res.* **74**, 778.

Daily, W.D.: 1973, Alfvén wave refraction by interplanetary inhomogeneities. *J. Geophys. Res.* **78**, 2043.

Dal Lago, A., Gonzalez, W.D., Balmaceda, L.A., Vieira, L.E., Echer, E., Guarnieri, F.L., Santos, J., Da Silva, M.R., De Lucas, A., Clua de Gonzalez, A.L., et al.: 2006, The 17–22 October (1999) solar-interplanetary-geomagnetic event: Very intense geomagnetic storm associated with a pressure balance between interplanetary coronal mass ejection and a high-speed stream. *J. Geophys. Res.: Space Physics* **111**.

Dasso, S., Milano, L., Matthaeus, W., Smith, C.: 2005, Anisotropy in fast and slow solar wind fluctuations. *Astrophys. J.* **635**, L181.

Dasso, S., Mandrini, C.H., Démoulin, P., Luoni, M.L.: 2006, A new model-independent method to compute magnetic helicity in magnetic clouds. *Astron. Astrophys.* **455**, 349.

Dobrowolny, M., Mangeney, A., Veltri, P.: 1980, Fully developed anisotropic hydromagnetic turbulence in interplanetary space. *Phys. Rev. Lett.* **45**, 144.

D'Amicis, R., Bruno, R.: 2015, On the origin of highly Alfvénic slow solar wind. *Astrophys. J.* **805**, 84.

D'amicis, R., Matteini, L., Bruno, R.: 2019, On the slow solar wind with high Alfvénicity: from composition and microphysics to spectral properties. *Mon. Not. Roy. Astron. Soc.* **483**, 4665.

Echer, E., Gonzalez, W., Tsurutani, B.: 2008, Interplanetary conditions leading to superintense geomagnetic storms (Dst$\leq$- 250 nT) during solar cycle 23. *Geophys. Res. Lett.* **35**.

Elsasser, W.M.: 1950, The hydromagnetic equations. *Phys. Rev.* **79**, 183.

Feldman, U., Landi, E., Schwadron, N.: 2005, On the sources of fast and slow solar wind. *J. Geophys. Res.: Space Physics* **110**.

Gekelman, W.: 1999, Review of laboratory experiments on Alfvén waves and their relationship to space observations. *J. Geophys. Res., Space Phys.* **104**, 14417. DOI.

Gekelman, W.: 2003, Laboratory experiments on Alfvén waves caused by rapidly expanding plasmas and their relationship to space phenomena. *J. Geophys. Res.* **108**. DOI.

Gosling, J., Pizzo, V.: 1999, Formation and evolution of corotating interaction regions and their three dimensional structure. In: *Corotating Interaction Regions*, Springer, Berlin, 21.

Gosling, J., Tian, H., Phan, T.: 2011, Pulsed Alfven waves in the solar wind. *Astrophys. J. Lett.* **737**, L35.

Gosling, J., Skoug, R., McComas, D., Smith, C.: 2005, Magnetic disconnection from the Sun: Observations of a reconnection exhaust in the solar wind at the heliospheric current sheet. *Geophys. Res. Lett.* **32**.

Gosling, J., McComas, D., Roberts, D., Skoug, R.: 2009, A one-sided aspect of Alfvénic fluctuations in the solar wind. *Astrophys. J.* **695**, L213.

Hasegawa, A., Chen, L.: 1974, Plasma heating by Alfvén-wave phase mixing. *Phys. Rev. Lett.* **32**, 454.

Hasegawa, A., Chen, L.: 1975, Kinetic process of plasma heating due to Alfvén wave excitation. *Phys. Rev. Lett.* **35**, 370.

Heinemann, S.G., Temmer, M., Farrugia, C.J., Dissauer, K., Kay, C., Wiegelmann, T., Dumbović, M., Veronig, A.M., Podladchikova, T., Hofmeister, S.J., et al.: 2019, CME–HSS interaction and characteristics tracked from Sun to Earth. *Solar Phys.* **294**, 1.

Hellinger, P., Trávníček, P.M.: 2008, Oblique proton fire hose instability in the expanding solar wind: Hybrid simulations. *J. Geophys. Res.: Space Physics* **113**.

Hellinger, P., Trávníček, P.M.: 2011, Proton core-beam system in the expanding solar wind: Hybrid simulations. *J. Geophys. Res.: Space Physics* **116**.

Hellinger, P., Trávníček, P.M.: 2013, Protons and alpha particles in the expanding solar wind: hybrid simulations. *J. Geophys. Res., Space Phys.* **118**, 5421.

Hinton, P., Bagenal, F., Bonfond, B.: 2019, Alfvén wave propagation in the Io plasma torus. *Geophys. Res. Lett.* **46**, 1242.

Hollweg, J.V.: 1975, Alfvén wave refraction in high-speed solar wind streams. *J. Geophys. Res.* **80**, 908.

Hollweg, J.V., Kaghashvili, E.K.: 2011, Alfvén waves in shear flows revisited. *Astrophys. J.* **744**, 114.

Hui, C.-H., Seyler, C.: 1992, Electron acceleration by Alfvén waves in the magnetosphere. *J. Geophys. Res., Space Phys.* **97**, 3953.

Hull, A., Chaston, C., Bonnell, J., Wygant, J.R., Kletzing, C., Reeves, G., Gerrard, A.: 2019, Dispersive Alfvén wave control of O+ ion outflow and energy densities in the inner magnetosphere. *Geophys. Res. Lett.* **46**, 8597.

Hundhausen, A.: 1999, Coronal mass ejections. In: *The Many Faces of the Sun*, Springer, Berlin, 143.

Jacques, S.: 1977, Momentum and energy transport by waves in the solar atmosphere and solar wind. *Astrophys. J.* **215**, 942.

Jess, D.B., Mathioudakis, M., Erdélyi, R., Crockett, P.J., Keenan, F.P., Christian, D.J.: 2009, Alfvén waves in the lower solar atmosphere. *Science* **323**, 1582.

Johnson, J.R., Cheng, C.: 1997, Kinetic Alfvén waves and plasma transport at the magnetopause. *Geophys. Res. Lett.* **24**, 1423.

Keiling, A.: 2009, Alfvén waves and their roles in the dynamics of the Earth's magnetotail: a review. *Space Sci. Rev.* **142**, 73.

Keiling, A., Thaller, S., Wygant, J., Dombeck, J.: 2019, Assessing the global Alfvén wave power flow into and out of the auroral acceleration region during geomagnetic storms. *Sci. Adv.* **5**, eaav8411.

Kennel, C., Edmiston, J., Hada, T.: 1985, *A Quarter Century of Collisionless Shock Research. Geophysical Monograph Series*, **34**, Am. Geophys. Union, Washington, 1.

Kilpua, E., Koskinen, H.E., Pulkkinen, T.I.: 2017, Coronal mass ejections and their sheath regions in interplanetary space. *Living Rev. Solar Phys.* **14**, 1.

Kilpua, E., Li, Y., Luhmann, J., Jian, L., Russell, C.: 2012, On the relationship between magnetic cloud field polarity and geoeffectiveness. *Ann. Geophys.* **30**(7), 1037. DOI.

Kilpua, E., Balogh, A., Von Steiger, R., Liu, Y.: 2017, Geoeffective properties of solar transients and stream interaction regions. *Space Sci. Rev.* **212**, 1271.

Kopp, R., Pneuman, G.: 1976, Magnetic reconnection in the corona and the loop prominence phenomenon. *Solar Phys.* **50**, 85.

Krieger, A., Timothy, A., Roelof, E.: 1973, A coronal hole and its identification as the source of a high velocity solar wind stream. *Solar Phys.* **29**, 505.

Lavraud, B., Ruffenach, A., Rouillard, A.P., Kajdic, P., Manchester, W.B., Lugaz, N.: 2014, Geo-effectiveness and radial dependence of magnetic cloud erosion by magnetic reconnection. *J. Geophys. Res., Space Phys.* **119**, 26.

Lepping, R., Burlaga, L., Szabo, A., Ogilvie, K., Mish, W., Vassiliadis, D., Lazarus, A., Steinberg, J., Farrugia, C.J., Janoo, L., et al.: 1997, The Wind magnetic cloud and events of October 18–20, 1995: interplanetary properties and as triggers for geomagnetic activity. *J. Geophys. Res., Space Phys.* **102**, 14049.

Levy, R., Petschek, H., Siscoe, G.: 1964, Aerodynamic aspects of the magnetospheric flow. *AIAA J.* **2**, 2065.

Li, H., Wang, C., Chao, J., Hsieh, W.: 2016, A new approach to identify interplanetary Alfvén waves and to obtain their frequency properties. *J. Geophys. Res., Space Phys.* **121**, 42.

Lysak, R.: 2004, Magnetosphere-ionosphere coupling by Alfvén waves at midlatitudes. *J. Geophys. Res.: Space Physics* **109**.

Malara, F., Primavera, L., Veltri, P.: 2001, Nonlinear evolution of the parametric instability: numerical predictions versus observations in the heliosphere. *Nonlinear Process. Geophys.* **8**, 159.

Manchester, W.B. IV, Gombosi, T.I., Roussev, I., Ridley, A., De Zeeuw, D.L., Sokolov, I., Powell, K.G., Tóth, G.: 2004, Modeling a space weather event from the Sun to the Earth: CME generation and interplanetary propagation. *J. Geophys. Res.: Space Physics* **109**.

Mann, I., Kimura, H.: 2000, Interstellar dust properties derived from mass density, mass distribution, and flux rates in the heliosphere. *J. Geophys. Res., Space Phys.* **105**, 10317.

Marsch, E., Mangeney, A.: 1987, Ideal MHD equations in terms of compressive Elsässer variables. *J. Geophys. Res., Space Phys.* **92**, 7363.

Marsch, E., Tu, C.-Y.: 1993, Modeling results on spatial transport and spectral transfer of solar wind Alfvénic turbulence. *J. Geophys. Res., Space Phys.* **98**, 21045.

Mathioudakis, M., Jess, D.B., Erdelyi, R.: 2013, Alfvén waves in the solar atmosphere. *Space Sci. Rev.* **175**, 1.

Matteini, L., Landi, S., Hellinger, P., Velli, M.: 2006, Parallel proton fire hose instability in the expanding solar wind: Hybrid simulations. *J. Geophys. Res.: Space Physics* **111**.

Matthaeus, W.H., Goldstein, M.L.: 1982, Stationarity of magnetohydrodynamic fluctuations in the solar wind. *J. Geophys. Res., Space Phys.* **87**, 10347.

Matthaeus, W.H., Minnie, J., Breech, B., Parhi, S., Bieber, J., Oughton, S.: 2004, Transport of cross helicity and radial evolution of Alfvénicity in the solar wind. *Geophys. Res. Lett.* **31**.

Meng, X., Tsurutani, B.T., Mannucci, A.J.: 2019, The solar and interplanetary causes of superstorms (minimum Dst$\leq$- 250 nT) during the space age. *J. Geophys. Res., Space Phys.* **124**, 3926.

National Research Council: 2008, *Severe Space Weather Events: Understanding Societal and Economic Impacts: A Workshop Report*, National Academies Press, Washington, DC. DOI.

Neugebauer, M.: 1981, Observations of solar-wind helium. *Fundam. Cosm. Phys.* **7**, 131.

Parker, E.: 1965, Dynamical theory of the solar wind. *Space Sci. Rev.* **4**, 666.

Perrone, D., D'amicis, R., De Marco, R., Matteini, L., Stansby, D., Bruno, R., Horbury, T.: 2020, Highly Alfvénic slow solar wind at 0.3 au during a solar minimum: Helios insights for Parker Solar Probe and Solar Orbiter. *Astron. Astrophys.* **633**, A166.

Petschek, H.E.: 1964, Magnetic field annihilation. In: *AAS-NASA Symposium on the Physics of Solar Flares: Proceedings of a Symposium Held at the Goddard Space Flight 50 Center, Greenbelt, Maryland, October 28 – 30, 1963. NASA SP-50*. Scientific and Technical Information Division, Washington DC, 425.

Raghav, A.N., Kule, A.: 2018, The first in situ observation of torsional Alfvén waves during the interaction of large-scale magnetic clouds. *Mon. Not. Roy. Astron. Soc. Lett.* **476**, L6.

Raghav, A.N., Choraghe, K., Shaikh, Z.I.: 2019, The cause of an extended recovery from an ICME-induced extreme geomagnetic storm: a case study. *Mon. Not. Roy. Astron. Soc.* **488**, 910.

Raghav, A.N., Kule, A., Bhaskar, A., Mishra, W., Vichare, G., Surve, S.: 2018, Torsional Alfvén wave embedded ICME magnetic cloud and corresponding geomagnetic storm. *Astrophys. J.* **860**, 26.

Raghav, A., Dhamane, O., Azmi, N., Manjrekar, A., Panchal, U., Ghag, K., Telloni, D., D'Amicis, R., Tari, P., Gurav, A., et al.: 2022a, First in-situ observation of surface Alfvén waves in ICME flux rope. preprint arXiv.

Raghav, A., Shaikh, Z., Dhamane, O., Ghag, K., Tari, P., Panchal, U.: 2022b, In-situ observation of Alfv'en waves in Icme shock-sheath indicates existence of Alfv'enic turbulence. preprint arXiv.

Riley, P., Crooker, N.: 2004, Kinematic treatment of coronal mass ejection evolution in the solar wind. *Astrophys. J.* **600**, 1035.

Riley, P., Sonett, C.P., Tsurutani, B.T., Balogh, A., Forsyth, R.J., Hoogeveen, G.W.: 1996a, Properties of arc-polarized Alfvén waves in the ecliptic plane: Ulysses observations. *J. Geophys. Res., Space Phys.* **101**, 19987. DOI.

Riley, P., Sonett, C., Tsurutani, B., Balogh, A., Forsyth, R., Hoogeveen, G.: 1996b, Properties of arc-polarized Alfvén waves in the ecliptic plane: Ulysses observations. *J. Geophys. Res., Space Phys.* **101**, 19987.

Roberts, D.A., Goldstein, M.L., Matthaeus, W.H., Ghosh, S.: 1992, Velocity shear generation of solar wind turbulence. *J. Geophys. Res., Space Phys.* **97**, 17115.

Roberts, D., Goldstein, M., Klein, L., Matthaeus, W.: 1987, Origin and evolution of fluctuations in the solar wind: Helios observations and Helios-Voyager comparisons. *J. Geophys. Res., Space Phys.* **92**, 12023.

Rodriguez, L., Masías-Meza, J.J., Dasso, S., Démoulin, P., Zhukov, A., Gulisano, A.M., Mierla, M., Kilpua, E., West, M., Lacatus, D., et al.: 2016, Typical profiles and distributions of plasma and magnetic field parameters in magnetic clouds at 1 AU. *Solar Phys.* **291**, 2145.

Ruffenach, A., Lavraud, B., Owens, M.J., Sauvaud, J.-A., Savani, N., Rouillard, A., Démoulin, P., Foullon, C., Opitz, A., Fedorov, A., et al.: 2012, Multispacecraft observation of magnetic cloud erosion by magnetic reconnection during propagation. *J. Geophys. Res.: Space Physics* **117**.

Ruffenach, A., Lavraud, B., Farrugia, C.J., Démoulin, P., Dasso, S., Owens, M.J., Sauvaud, J.-A., Rouillard, A., Lynnyk, A., Foullon, C., et al.: 2015, Statistical study of magnetic cloud erosion by magnetic reconnection. *J. Geophys. Res., Space Phys.* **120**, 43.

Schrijver, C.J., Siscoe, G.L.: 2010, *Heliophysics: Space Storms and Radiation: Causes and Effects*, Cambridge University Press, Cambridge.

Shaikh, Z.I., Raghav, A., Vichare, G.: 2019, Coexistence of a planar magnetic structure and an Alfvén wave in the shock-sheath of an interplanetary coronal mass ejection. *Mon. Not. Roy. Astron. Soc.* **490**, 1638.

Shaikh, Z.I., Raghav, A., Vichare, G., Bhaskar, A., Mishra, W., Choraghe, K.: 2019, Concurrent effect of Alfvén waves and planar magnetic structure on geomagnetic storms. *Mon. Not. Roy. Astron. Soc.* **490**, 3440.

Shi, C., Velli, M., Tenerani, A., Rappazzo, F., Réville, V.: 2020, Propagation of Alfvén waves in the expanding solar wind with the fast–slow stream interaction. *Astrophys. J.* **888**, 68.

Singer, H., Southwood, D., Walker, R., Kivelson, M.: 1981, Alfvén wave resonances in a realistic magnetospheric magnetic field geometry. *J. Geophys. Res., Space Phys.* **86**, 4589.

Singh, Y., et al.: 2009, Geoeffectiveness of magnetic cloud, shock/sheath, interaction region, high-speed stream and their combined occurrence. *Planet. Space Sci.* **57**, 318.

Stasiewicz, K., Bellan, P., Chaston, C., Kletzing, C., Lysak, R., Maggs, J., Pokhotelov, O., Seyler, C., Shukla, P., Stenflo, L., et al.: 2000, Small scale Alfvénic structure in the aurora. *Space Sci. Rev.* **92**, 423.

Telloni, D., D'Amicis, R., Bruno, R., Perrone, D., Sorriso-Valvo, L., Raghav, A.N., Choraghe, K.: 2021, Alfvénicity-related long recovery phases of geomagnetic storms: a space weather perspective. *Astrophys. J.* **916**, 64.

Tomczyk, S., McIntosh, S., Keil, S., Judge, P., Schad, T., Seeley, D., Edmondson, J.: 2007, Alfvén waves in the solar corona. *Science* **317**, 1192.

Tsubouchi, K.: 2009, Alfvén wave evolution within corotating interaction regions associated with the formation of magnetic holes/decreases. *J. Geophys. Res.: Space Physics* **114**.

Tsurutani, B.T., Gonzalez, W.D.: 1987, The cause of high-intensity long-duration continuous AE activity (HILDCAAs): interplanetary Alfvén wave trains. *Planet. Space Sci.* **35**, 405.

Tsurutani, B.T., Hajra, R.: 2022, Extremely slow (V sw< 300 km s- 1) Solar winds (ESSWs) at 1 au: causes of extreme geomagnetic quiet at Earth. *Astrophys. J.* **936**, 155.

Tsurutani, B.T., Gonzalez, W.D., Tang, F., Akasofu, S.I., Smith, E.J.: 1988, Origin of interplanetary southward magnetic fields responsible for major magnetic storms near solar maximum (1978 – 1979). *J. Geophys. Res., Space Phys.* **93**, 8519.

Tsurutani, B.T., Gonzalez, W.D., Tang, F., Lee, Y.T.: 1992, Great magnetic storms. *Geophys. Res. Lett.* **19**, 73.

Tsurutani, B.T., Gonzalez, W.D., Gonzalez, A.L., Tang, F., Arballo, J.K., Okada, M.: 1995a, Interplanetary origin of geomagnetic activity in the declining phase of the solar cycle. *J. Geophys. Res., Space Phys.* **100**, 21717.

Tsurutani, B.T., Ho, C.M., Arballo, J.K., Goldstein, B.E., Balogh, A.: 1995b, Large amplitude IMF fluctuations in corotating interaction regions: Ulysses at midlatitudes. *Geophys. Res. Lett.* **22**, 3397.

Tsurutani, B.T., Ho, C., Arballo, J., Smith, E., Goldstein, B., Neugebauer, M., Balogh, A., Feldman, W.: 1996, Interplanetary discontinuities and Alfvén waves at high heliographic latitudes: Ulysses. *J. Geophys. Res., Space Phys.* **101**, 11027.

Tsurutani, B.T., Gonzalez, W.D., Gonzalez, A.L., Guarnieri, F.L., Gopalswamy, N., Grande, M., Kamide, Y., Kasahara, Y., Lu, G., Mann, I., et al.: 2006a, Corotating solar wind streams and recurrent geomagnetic activity: a review. *J. Geophys. Res.: Space Physics* **111**.

Tsurutani, B.T., McPherron, R., Gonzalez, W., Lu, G., Sobral, J.H., Gopalswamy, N.: 2006b, *Recurrent Magnetic Storms: Corotating Solar Wind Streams* **167**, Am. Geophys. Union, Washington.

Tsurutani, B.T., Echer, E., Guarnieri, F.L., Gonzalez, W.D.: 2011a, The properties of two solar wind high speed streams and related geomagnetic activity during the declining phase of solar cycle 23. *J. Atmos. Solar-Terr. Phys.* **73**, 164.

Tsurutani, B.T., Lakhina, G.S., Sen, A., Hellinger, P., Glassmeier, K.-H., Mannucci, A.: 2017, Alfvenic turbulence in high speed solar wind streams: hints from comet plasma turbulence.

Tsurutani, B.T., Lakhina, G.S., Sen, A., Hellinger, P., Glassmeier, K.-H., Mannucci, A.J.: 2018, A review of Alfvénic turbulence in high-speed solar wind streams: hints from cometary plasma turbulence. *J. Geophys. Res., Space Phys.* **123**, 2458.

Tsurutani, B., Gonzalez, W., Zhou, X.-Y., Lepping, R., Bothmer, V.: 2004, Properties of slow magnetic clouds. *J. Atmos. Solar-Terr. Phys.* **66**, 147.

Tsurutani, B., Lakhina, G., Verkhoglyadova, O.P., Gonzalez, W., Echer, E., Guarnieri, F.: 2011b, A review of interplanetary discontinuities and their geomagnetic effects. *J. Atmos. Solar-Terr. Phys.* **73**, 5.

Tu, C.-Y., Marsch, E., Thieme, K.: 1989, Basic properties of solar wind MHD turbulence near 0.3 AU analyzed by means of Elsässer variables. *J. Geophys. Res., Space Phys.* **94**, 11739.

Verkhoglyadova, O., Tsurutani, B., Mannucci, A., Mlynczak, M., Hunt, L., Runge, T.: 2013, Variability of ionospheric TEC during solar and geomagnetic minima (2008 and 2009): external high speed stream drivers. *Ann. Geophys.* **31**(2), 263. DOI.

Von Steiger, R., Schwadron, N., Fisk, L., Geiss, J., Gloeckler, G., Hefti, S., Wilken, B., Wimmer-Schweingruber, R., Zurbuchen, T.: 2000, Composition of quasi-stationary solar wind flows from Ulysses/Solar wind ion composition spectrometer. *J. Geophys. Res., Space Phys.* **105**, 27217.

Vršnak, B., Temmer, M., Veronig, A.M.: 2007, Coronal holes and solar wind high-speed streams: I. Forecasting the solar wind parameters. *Solar Phys.* **240**, 315.

Vršnak, B., Ruždjak, V., Rompolt, B., Roša, D., Zlobec, P.: 1993, Kinematics and evolution of twist in the eruptive prominence of August 18, 1980. *Solar Phys.* **146**, 147.

Wang, X., He, J., Tu, C., Marsch, E., Zhang, L., Chao, J.-K.: 2012, Large-amplitude Alfvén wave in interplanetary space: the WIND spacecraft observations. *Astrophys. J.* **746**, 147.

Wang, Y., Xue, X., Shen, C., Ye, P., Wang, S., Zhang, J.: 2006, Impact of major coronal mass ejections on geospace during 2005 September 7-13. *Astrophys. J.* **646**, 625.

Wang, Z., Feng, X., Zheng, J.: 2019, Multispacecraft observation of unidirectional and bidirectional Alfvén waves within large-scale magnetic clouds. *Astrophys. J. Lett.* **887**, L18.

Webb, D.F., Howard, T.A.: 2012, Coronal mass ejections: observations. *Living Rev. Solar Phys.* **9**, 1.

Yang, L., Chao, J.: 2013, Alfvén waves in the solar wind. *Chin. J. Space Sci* **33**, 353.

Yang, L., Lee, L., Chao, J., Hsieh, W., Luo, Q., Li, J., Shi, J., Wu, D.: 2016, Observational evidence for the relationship between Walén slope and amplitude ratio of inward to outward Alfvén waves in the solar wind. *Astrophys. J.* **817**, 178.

Zhao, X., Dryer, M.: 2014, Current status of CME/shock arrival time prediction. *Space Weather* **12**, 448.

Zurbuchen, T.H., Richardson, I.G.: 2006, In-situ solar wind and magnetic field signatures of interplanetary coronal mass ejections. In: *Coronal Mass Ejections*, Springer, Berlin, 31.